ACS SENSORS

pubs.acs.org/acssensors

Article

# BioChemPen for a Rapid Analysis of Compounds Supported on Solid Surfaces

Yu-Ting Chao, Gurpur Rakesh D. Prabhu, Kai-Chiang Yu, Jia-You Syu, and Pawel L. Urban*

Cite This: *ACS Sens.* 2021, 6, 3744–3752

Read Online

ACCESS | Metrics & More | Article Recommendations | Supporting Information

**ABSTRACT:** We present BioChemPen, a portable wireless biosensor device for rapid analysis of substances adsorbed on solid surfaces. The device takes advantage of (bio)luminescent reactions taking place in a hydrogel matrix. In a typical embodiment, the active element of this device is a hydrogel disk (chemotransducer) containing enzyme(s), electrolyte solution, and all of the necessary substrates. When the hydrogel is exposed to a solid sample surface containing the target analyte, light is produced. A photoresistor (phototransducer), placed in close proximity to the hydrogel disk, detects the light. The operation of the BioChemPen is enabled by a MicroPython PyBoard microcontroller board and other low-cost electronic modules. The obtained results are immediately uploaded to the Internet cloud. In one application, we demonstrate an analysis of hypochlorite-containing cleaning agents present on the surfaces of daily use objects by an assay based on hydrogel embedded with luminol and hydrogen peroxide. In another application, we use hydrogel embedded with luciferin, luciferase, and pyruvate kinase to detect adenosine triphosphate (ATP), and adenosine diphosphate (ADP), and link the ATP content with meat freshness. Lastly, we demonstrate the detection of organophosphate pesticides present on vegetables with the hydrogel containing acetylcholinesterase, choline oxidase, and horseradish peroxidase. The limits of detection for sodium hypochlorite, ATP, ADP, and chlorpyrifos-methyl (a pesticide) were $7.95 \times 10^{-11}$, $2.73 \times 10^{-13}$, $2.35 \times 10^{-12}$, and $2.59 \times 10^{-10}$ mol mm$^{-2}$, respectively.

**KEYWORDS:** *bleach, hydrogel, Internet-of-things, meat freshness, microcontroller, nucleotides, pesticides, portable biosensors*



Portable biosensors have several advantages, including ease-of-use, operability in resource-limited settings, low consumption of samples and reagents, and, most importantly, rapid and real-time analysis without sample preparation.[1−3] Due to these advantages, handheld biosensors are applicable across various fields, including clinical diagnostics,[2] therapeutic drug monitoring,[4] environmental water monitoring,[5] and food quality control.[1] Moreover, recent advances in wireless technologies (Wi-Fi and Bluetooth) have led to the proliferation of wireless analytical devices.[6] Wireless devices with Internet connectivity are very convenient because they enable real-time data transmission to the cloud and remote monitoring of processes.

Monitoring the cleanliness of surfaces for the absence of microbes, pesticides, or other contaminants is important in the food industry,[7] hospitals,[8] and forensic laboratories,[9] to name a few application areas. For instance, the processing and packaging of food items in the food industry are usually done on open surfaces of tables, shelves, conveyors, and sinks. Food products placed on open and unclean surfaces can contaminate the food. On the other hand, frequently touched surfaces of publicly shared equipment (contaminated with pathogens) can easily spread contagious diseases (e.g., COVID-19[10]). There exist several methods to verify surface cleanliness;[11] for example, sampling microbes onto an agar contact plate[12] and vacuuming surfaces to collect microbes onto a growth media.[13] Other methods for evaluating the cleanliness of solid surfaces include swabbing surfaces to collect chemical residues or microorganisms for analysis by means of a luminometer,[14] a real-time polymerase chain reaction machine,[15] or a mass spectrometer.[16] Analysis of a solid surface for the presence or absence of certain harmful species (e.g., microorganisms, pesticides, explosives) imposes several requirements: it should be fast, convenient, easy, and accurate.

Food quality is a fundamental requirement of consumers, and there is a growing need for food quality assessment. Disinfecting the surfaces of fresh produce with bleach is convenient.[17] Therefore, some food industries disinfect the surfaces of perishables using sodium hypochlorite-treated water.[18,19] To avoid ingestion of residual hypochlorite by consumers, it is necessary to rule out the presence of excessive amounts of this

**Received:** July 20, 2021
**Accepted:** September 8, 2021
**Published:** September 23, 2021





https://doi.org/10.1021/acssensors.1c01540
*ACS Sens.* 2021, 6, 3744–3752

chemical on foodstuffs. On the other hand, it is also important to evaluate food freshness. There exist several analytical approaches to verify meat freshness, including the use of Raman spectroscopy,[20] hyperspectral imaging,[21] and portable optoelectronic nose.[22] Detection of adenosine triphosphate (ATP) is another viable strategy for the assessment of meat freshness[23] because ATP is a major carrier of chemical energy in living organisms and plays a major role in cellular metabolism.[24]

The presence of pesticides on the surfaces of eatables is another potential health risk to the consumers.[25] Based on the chemical nature, pesticides can be classified into two groups, organic and inorganic. Inorganic pesticides are used very rarely, whereas organic pesticides are used widely and are an extremely large group of compounds. The residual organic pesticides detected on the surfaces of fruits and vegetables include organophosphate pesticides, organochlorine pesticides, and pyrethroids.[26] Liquid chromatography−mass spectrometry (MS)[26] and gas chromatography−MS[27] systems can be used to detect pesticides. However, MS-based techniques require bulky instruments and experts to develop methods and perform analyses.

Hydrogel is a three-dimensional (3D) network of natural or synthetic hydrophilic polymers held together by chemical cross-linking chains.[28,29] Hydrogels swell when placed in water, and they absorb large amounts of water while preserving their 3D structure.[28,29] Due to the significant water content, hydrogels are flexible and biocompatible. In addition, they have low toxicity; therefore, they can protect embedded cells and/or cellular components, such as proteins (enzymes) and peptides from harsh surroundings.[28,30] For these reasons, hydrogels find applications in various fields, including drug delivery, food additives, biomedicine, and biosensors.[31,32]

Here, we introduce an in-house-built, hydrogel-based, handheld optoelectronic biosensor that can detect several analytes supported on solid surfaces based on different gel-phase luminescent reactions and upload the analysis results to the Internet cloud. The device, named "BioChemPen" (Figure 1), incorporates a microcontroller board (MCB) for data collection and Internet connectivity and the necessary circuitry in a 3D-printed casing. It is powered by rechargeable lithium-ion batteries. The 3D-printed casing of the device includes a disposable unit containing the hydrogel (with the reagents) and a photoresistor to detect the light produced in the gel-phase luminescent reactions (Figure S1).

## EXPERIMENTAL SECTION

**Design and Construction of BioChemPen.** The casing of the BioChemPen (Figures S2 and S3) was designed using Inventor Professional 2020 software (version 2020.0.1; Autodesk, San Rafael, CA) and printed using acrylonitrile-butadiene-styrene (ABS) on a 3D printer (ZRapid, SLA550; Chih-Teng 3D Technology, New Taipei City, Taiwan). Four screws (M2 × 35 mm, nickel, part no. 6AB0011; Kinsten, Hsinchu City, Taiwan) and nuts (M2, nickel, part no. 6BA001; Kinsten, Hsinchu City, Taiwan) were used to fix the parts A and B of the main casing together. The 3D-printed casing also includes a cartridge (parts C and D). The cartridge incorporates a photoresistor (part no. GL5528, spectral response peak: 540 nm, 8−20 kΩ, ⌀ = 5.1 ± 0.2 mm mm; Centenary Materials, Hsinchu, Taiwan) and an agarose hydrogel disk (⌀ = 0.3 cm, $h$ = 0.2 cm) containing reagents (see below). Similar to a laboratory micropipette that incorporates a plunger button to dispose of the tip, the BioChemPen also incorporates a plunger button with a piston (parts E and F) to enable ejection of the cartridge (parts C and D) after analysis. To perform the next analysis, one needs to attach a new cartridge. In addition, for the baseline measurement in real sample tests, we printed a cap (Figure S4; 3D printer: UP Plus 2, 3DP-

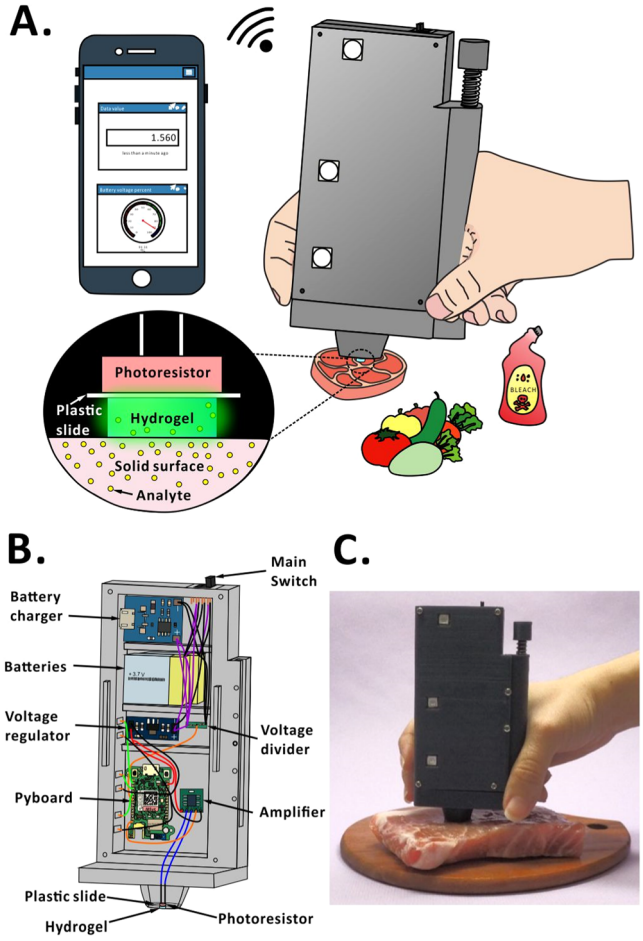


**Figure 1.** BioChemPen setup: (A) schematic illustration of the common detection method; (B) simplified diagram depicting the internal circuits; (C) illustrative photograph of the BioChemPen (without the optional light-proof shield, cf. Figure S5).

14-4D; Beijing TierTime Technology, Beijing, China; material: ABS). To reduce the influence of ambient light during analysis, we covered the lower part of the BioChemPen with a light-proof shield made of aluminum foil (∼7 layers) strengthened by black tape (Figure S5). The design of BioChemPen has evolved over several different versions (Figure S6) before arriving at the final design of one casing for the incorporation of all the electronics and chemical reagents necessary to perform an analysis.

The internal circuitry of the BioChemPen (Figures 1B, 2, and S3B) includes a MicroPython PyBoard D-series MCB (model: SF6W, with STM32F767VIT microcontroller unit and Murata 1DX module for Wi-Fi/Bluetooth; micropython.org, Cambridge, U.K.) with an associated program written in MicroPython[33] (Python language optimized for microcontrollers) for data collection and Wi-Fi connectivity (see workflow in Figure S7); an amplifier printed circuit board (PCB; custom-made by Good Technology, Taichung, Taiwan; based on Figure S8) to amplify the signal from the photoresistor; a voltage regulator (part no. 95468; Centenary Materials, Hsinchu, Taiwan) to maintain a constant supply of 5 V to the MCB; two 3.7 V lithium-ion polymer rechargeable batteries (500 mAh; part no. 112766; Centenary Materials, Hsinchu, Taiwan) to power the device; a battery charger unit (with microUSB, 4.5−5.5 V, 1 A, 25 × 19 × 5 mm; part no. 98765; Centenary Materials, Hsinchu, Taiwan); and a voltage divider (resistors: 51 and 82 kΩ) between the batteries and the analog pin X4 of the MCB to determine the battery level. The device also incorporates a Main switch (slide switch with 8 pins, part no. 5065D; Kinsten, Hsinchu City, Taiwan) to switch between two modes: battery-charging mode and operation mode. In the operation mode, the two


https://doi.org/10.1021/acssensors.1c01540
ACS Sens. 2021, 6, 3744−3752

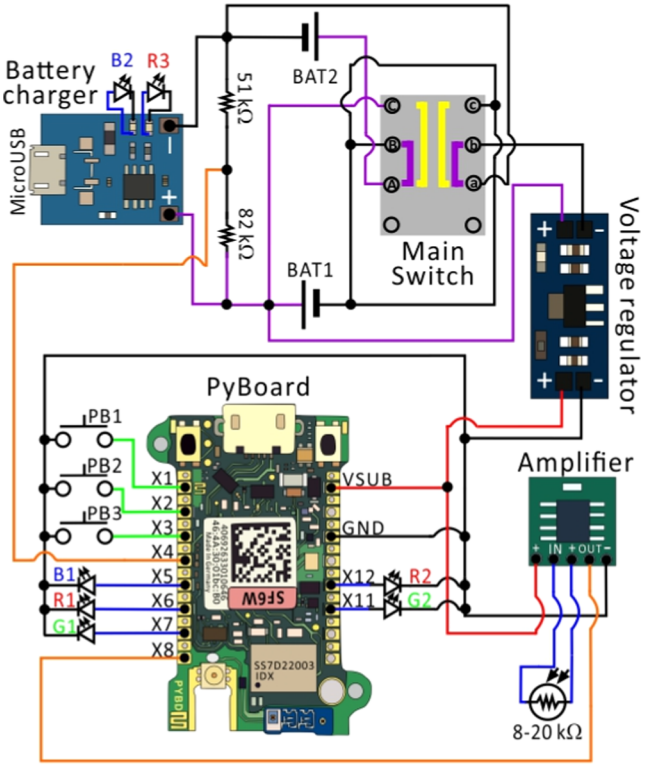


**Figure 2.** Circuit diagram of the BioChemPen. In the main switch, yellow brackets indicate charging mode, purple brackets indicate operation mode. Push buttons: PB1 to check battery level, PB2 to determine the baseline, and PB3 to initiate sample analysis. LEDs: R1, G1, and B1 to indicate battery level; R2 to indicate sample analysis; G2 to indicate baseline measurement; R3 to indicate battery-charging mode; and B2 to indicate a full battery.

batteries are connected in series to the voltage regulator to power the MCB and the amplifier PCB. In the battery-charging mode, the batteries are connected in parallel to charge the batteries. The device also incorporates three push buttons (rating: DC 12 V 50 mA; Kinsten, Hsinchu City, Taiwan) to enable the initiation of different functions (cf. Figures 2 and S3A, and source code in the Supporting Information): the first button (PB1; Battery button) to check the battery level, the second button (PB2; Baseline button) to determine the baseline, and the third button (PB3; Sample button) to initiate sample analysis. A multicolor LED (red−green−blue, 5050 SMD LED, part no. 100441; Centenary Materials, Hsinchu City, Taiwan), connected to the PyBoard, allows one to check the battery level. Lights of different colors appear for different battery levels: red, 0−53%; green, 54−87%; and blue, 88−100%. In addition, the device includes two more multicolor LEDs to indicate "operation mode" and "charging mode". The operation mode LED glows green during baseline measurement and red during sample analysis. The charging mode LED glows red while charging batteries and blue when the charging is complete.

The flash memory of the MCB contains three program files: "boot.py", "main.py", and "func.py" (cf. Supporting Information). The boot.py file runs upon powering the MCB and initiates the program in main.py, which, in turn, initiates the BioChemPen's operation program in the func.py file. It is possible to access these files (and modify the code) *via* a universal serial bus (USB) connection between the MCB and a personal computer (PC). However, the script in the main.py file and the circuit are specially designed to enable wireless access of the files (program and data files) in the MCB's flash memory (see Figure S9) following a prior transfer of the program files to the MCB's flash memory *via* USB. The final analysis results are uploaded to the cloud (ThingSpeak.com, MathWorks, Natick, MA; Figure S10) immediately after the analysis so that one can easily check the results on a smartphone.

**Preparation of Hydrogel Disks.** To prepare the hydrogel disks for the detection of sodium hypochlorite, first, agarose solution was prepared by heating agarose suspension in water (22 g $L^{-1}$) to ∼90 °C in a water bath until the formation of a transparent solution (Figure S11A). Further, the agarose solution was cooled to 50 °C (Figure S11B). Then, 1 mL of 0.088 M luminol solution [prepared in an electrolyte at pH 13 (0.145 M sodium hydroxide and 0.05 M potassium chloride)], 1 mL of 0.338 M hydrogen peroxide solution, and 2 mL of 22 g $L^{-1}$ cooled agarose solution were pipetted to a 50 mL plastic tube (Figure S11C), and the mixture was vortexed at 1600 rpm for 20 s. Subsequently, the mixture was transferred into a glass Petri dish (⌀ = 5 cm) and cooled to room temperature (∼22 ± 4 °C; Figure S11D). After ∼10 min, when the sol phase transformed to the gel phase, a glass tube (I.D., 0.3 cm) was used to cut disks (⌀ = 0.3 cm, $h$ = 0.2 cm) out of the hydrogel mass. Note that thinner disks would be too fragile to be handled manually. The hydrogel disks were then transferred into the cartridge of the BioChemPen with tweezers (Figure S11E). The average weight of twenty such hydrogel disks was 14.99 mg [relative standard deviation (RSD), 3.37%].

A similar protocol was followed while preparing hydrogel disks containing luciferase for the detection of ATP. However, the agarose solution was cooled to ∼40 °C before adding the enzyme to avoid enzyme deactivation. The final reagent solution (4 mL) consisted of 1 × $10^{-3}$ M magnesium sulfate, 2 × $10^{-4}$ M ethylenediaminetetraacetic acid (EDTA), 3.5 × $10^{-4}$ M luciferin, 4.85 × $10^{9}$ LU $mL^{-1}$ luciferase (0.01 μg per disk), Tris−HCl buffer at pH 8 (0.1 M Trizma base solution; pH adjusted with 2 M hydrochloric acid), and 7 g $L^{-1}$ agarose in water. Similarly, hydrogel disks for the detection of adenosine diphosphate (ADP) were prepared with the final reagent solution (4 mL) consisting of 1 × $10^{-3}$ M magnesium sulfate, 2 × $10^{-4}$ M EDTA, 3.5 × $10^{-4}$ M luciferin, 4.85 × $10^{9}$ LU $mL^{-1}$ luciferase (0.01 μg per disk), 1 × $10^{-3}$ M phosphoenolpyruvic acid monopotassium salt (PEP), 40 U $mL^{-1}$ pyruvate kinase (0.13 μg per disk), and 7 g $L^{-1}$ agarose in water. On the other hand, in the hydrogel disks for the detection of pesticide, the concentration of agarose was 7 g $L^{-1}$ (in water), and the final reagent solution (4 mL) consisted of 100 U $mL^{-1}$ acetylcholinesterase (AChE; 1.4 μg per disk), 20 U $mL^{-1}$ choline oxidase (ChOx; 6.0 μg per disk), and 108 U $mL^{-1}$ horseradish peroxidase (HRP; 0.57 μg per disk), all in 0.1 M phosphate buffer at pH 7.5, containing 2.0 mM EDTA and 0.1 M potassium chloride. After sampling the target surface, prior to analysis, the AChE-ChOx-HRP hydrogel disk was soaked in 10 μL of acetylcholine (Ach) solution (concentration: 0.25 M; pH: 8, adjusted using dilute sodium hydroxide) for 1 min, and soaked in 10 μL of luminol solution (concentration: 0.145 M; pH: 13; adjusted using 0.145 M sodium hydroxide and 0.05 M potassium chloride solution).

**Data Acquisition and Treatment.** The analog signal from the photoresistor is first amplified (∼11 times) by the amplifier PCB. For example, with an input voltage of 0.203 V to the amplifier PCB, the output voltage will be 2.235 V. The MCB is programmed to collect 20 data points per 100 ms, which are subsequently averaged to reduce the electronic noise. The MCB then converts the averaged analog values (0 to 4095) to voltage values (0−3.3 V). When the Baseline button (PB2) is pressed, the operation mode LED flickers the green light twice to indicate the start of the data acquisition process. Then, the green light remains on for 15 s as the baseline is recorded, and an average baseline value is calculated. The hydrogel disk can be pressed against a clean filter paper, a glass slide, or a 3D-printed cap (cf. Figure S4) to record the baseline. Upon pressing the Sample button (PB3), the operation mode LED flickers red light twice to indicate the start of the data acquisition process and the creation of a "data.txt" file. Subsequently, the program determines the corrected voltage by first converting the analog sensor values from negative to positive and then subtracting the baseline value from every data point (150 data points) obtained for the sample. The red light remains on for 15 s as the sample data is recorded, and the recorded data is saved in the data.txt file in the flash memory of the MCB. Lastly, the area under the curve from the time-dependent plot of corrected voltage (Figure S12) is calculated, and the result is uploaded onto the cloud (ThingSpeak.com).


https://doi.org/10.1021/acssensors.1c01540
ACS Sens. 2021, 6, 3744−3752

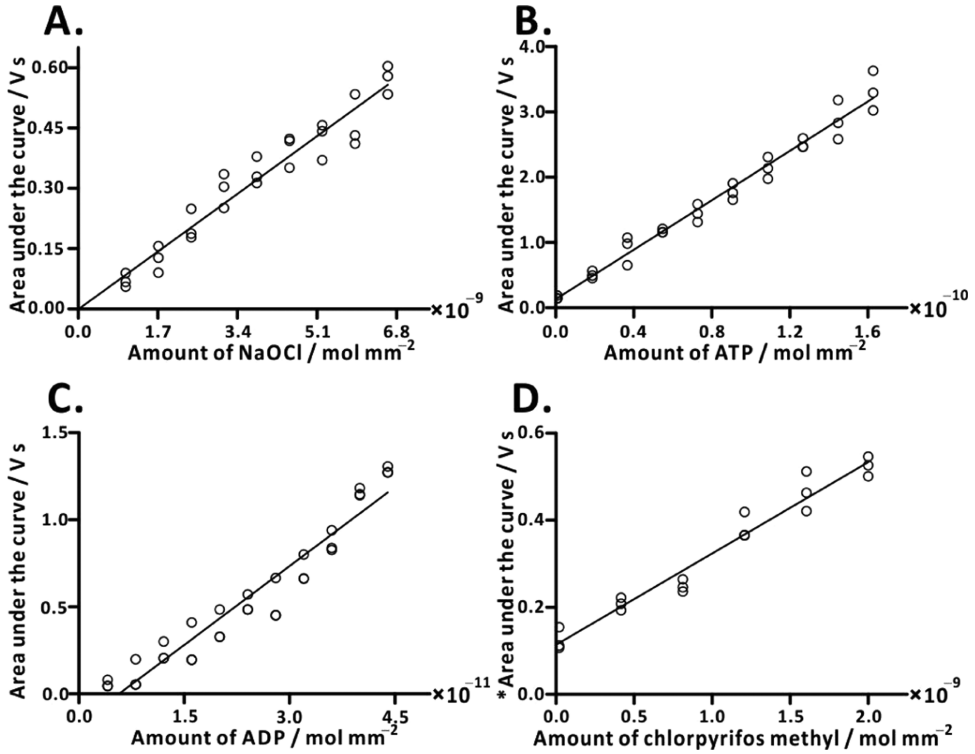


**Figure 3.** Calibration of BioChemPen with standards: (A) sodium hypochlorite; (B) ATP; (C) ADP; and (D) chlorpyrifos-methyl (*blank minus test sample). cf. Table 1.

Additional experimental details (chemicals and real samples) and a short video (Movie S1) demonstrating the operation of BioChemPen are provided in the Supporting Information.

## RESULTS AND DISCUSSION

**Proof-of-Concept: Detection of Bleach Residues Using Gel-Phase Luminol Chemiluminescent Reaction.** BioChemPen has been developed using inexpensive electronic modules and prototyping tools (cf. refs 34−37). The detachable cartridge integrates a chemotransducer (hydrogel disk) and an inexpensive phototransducer (photoresistor). The hydrogel matrix is convenient because it can store both low-molecular-weight substrates and macromolecular catalysts (enzymes). It also carries water required to solubilize the analytes adsorbed on the sampled solid surfaces and to provide a suitable reaction environment. The Wi-Fi-enabled device allows one to see the analysis result on a smartphone (Figure S13). The device has been optimized and tested in analyses of several real sample surfaces (daily use objects, meat, and vegetables) for the detection of sodium hypochlorite, ATP, ADP, or a pesticide. The early development of the BioChemPen was accompanied by a series of experiments, in which hydrogel disks with embedded chemicals (enzymes, substrates) were placed on the surface of filter paper containing the analytes, and the (bio)luminescence was captured by a digital camera (model: EM1; Olympus, Tokyo, Japan; Figure S14).

To optimize the parameters influencing the gel-phase luminescent reaction for the detection of sodium hypochlorite (Figure S1A),[38] hydrogel disks containing different concentrations of chemicals (luminol, hydrogen peroxide, agarose, and sodium hydroxide) were tested. Filter paper disks (⌀ = 2.8 cm), impregnated with freshly prepared standard sodium hypochlorite solution, were oven-dried at 60 °C for 7 min and used as test surfaces. The concentration of sodium hypochlorite on the surface of the filter paper disk was $3.11 \times 10^{-9}$ mol mm$^{-2}$. Based on the optimization results (Figure S15), hydrogel disks of the following chemical composition were chosen for the analyses: $2.2 \times 10^{-2}$ M luminol [prepared in an electrolyte at pH 13 (0.145 M sodium hydroxide and 0.05 M potassium chloride)], $8.45 \times 10^{-2}$ M hydrogen peroxide, and 11 g L$^{-1}$ agarose.

To characterize the described method, we prepared a calibration plot using different concentrations of sodium hypochlorite ($1.01 \times 10^{-9}$ to $6.61 \times 10^{-9}$ mol mm$^{-2}$; 9 levels) on filter paper disks (Figure 3A and Table 1; this narrow range was selected considering the anticipated concentrations in the real matrices). The limit of detection (LOD) and limit of quantification [LOQ; cf. formulae (1, 2, and 3) in the Supporting Information] for sodium hypochlorite on filter paper disks were $7.95 \times 10^{-11}$ and $2.65 \times 10^{-10}$ mol mm$^{-2}$, respectively. Furthermore, using filter paper disks impregnated with sodium hypochlorite solution ($1.71 \times 10^{-9}$ mol mm$^{-2}$), the repeatability [9.07%, RSD, $n$ = 10; on one day; cf. Table 1] and the reproducibility (7.52%, RSD, $n$ = 18; three replicates per day on six consecutive days) of the method were determined.

To demonstrate the applicability of the BioChemPen in analyses of real surfaces, the device was tested in the detection of bleach on a Paulownia wood surface and a western red cedar flooring material surface (Figure S16A,B). The wood surfaces were treated with sodium hypochlorite at two different concentrations [0.1% (w/w) and 0.06% (w/w)], which are in the order of the concentrations recommended for cleaning and disinfection of surfaces: 0.1% (effective against most pathogens) and 0.05% (effective against rotavirus).[39] In the case of western red cedar flooring material, we wiped the painted wood surface with the hypochlorite solution. In the case of Paulownia wood, we soaked the unpainted wood pieces in the hypochlorite solution for 10 min and dried them for about 4 h at room temperature (cf. Supporting Information). Subsequently, the


https://doi.org/10.1021/acssensors.1c01540
ACS Sens. 2021, 6, 3744−3752

Table 1. Analytical Performance of the BioChemPen[a]

| analyte | calibration equation ($A$/(V s); $C$/mol mm$^{-2}$) | $R^2$ | $S_{max}$ | $S_{blank}$ | $\sigma_{blank}$ | $C_l$ | LOD/mol mm$^{-2}$ | LOQ/mol mm$^{-2}$ | repeatability (RSD)/% ($n$ = 10) | reproducibility (RSD)/% ($n$ = 18; 6 days; each day $n$ = 3) |
|---|---|---|---|---|---|---|---|---|---|---|
| sodium hypochlorite | $A = (8.45 \times 10^{7} \pm 0.45 \times 10^{7})C - (0.001 \pm 0.018)$ | 0.932 | 0.0923 | −0.00182 | 0.00247 | $1.01 \times 10^{-9}$ | $7.95 \times 10^{-11}$ | $2.65 \times 10^{-10}$ | 9.07 | 7.52 |
| ATP | $A = (1.89 \times 10^{10} \pm 0.06 \times 10^{10})C + (0.131 \pm 0.054)$ | 0.975 | 0.111 | 0.00324 | 0.0135 | $7.24 \times 10^{-13}$ | $2.73 \times 10^{-13}$ | $9.09 \times 10^{-13}$ | 5.94 | 7.20 |
| ADP | $A = (3.02 \times 10^{10} \pm 0.15 \times 10^{10})C - (0.172 \pm 0.041)$ | 0.925 | 0.0997 | 0.00348 | 0.0184 | $4.09 \times 10^{-12}$ | $2.35 \times 10^{-12}$ | $7.84 \times 10^{-12}$ | 9.11 | 7.05 |
| pesticide (chlorpyrifos-methyl) | $A = (2.37 \times 10^{8} \pm 0.14 \times 10^{8})C + (0.074 \pm 0.015)$ | 0.935 | 0.194 | 0.0420 | 0.00657 | $2.00 \times 10^{-9}$ | $2.59 \times 10^{-10}$ | $8.64 \times 10^{-10}$ | 9.19 | 8.63 |

[a]For the corresponding calibration plots, see Figure 3 . To record the baseline, the BioChemPen's hydrogel tip was pressed against a clean filter paper disk (in the case of sodium hypochlorite, ATP, and ADP), and a clean glass slide (in the case of pesticide). LOD and LOQ were calculated using the formulae (1−3) described in the section "additional experimental details" in the Supporting Information.

BioChemPen's hydrogel disk was brought into contact with the hypochlorite-treated wooden surfaces for the detection of the target analyte. The results indicate that the BioChemPen can differentiate between the surfaces with and without hypochlorite treatment (Figure S17).

Furthermore, we tested the device on daily use objects (metal doorknob, wooden table, metal cabinet, and plastic chair) wiped with a diluted commercial bleach solution (0.02 L bleach mixed with 2 L water; cf. Supporting Information). Because the actual concentration of the commercial bleach solution was unknown (lack of clear labeling), and the tested surfaces had a different texture than the filter paper disks and test wood pieces, we slid the hydrogel tip of the BioChemPen over the testing surfaces (∼10 cm) to collect a sufficient amount of sodium hypochlorite for detection. The blank tests were done on the same surfaces but without any hypochlorite treatment. The chemiluminescence signals, obtained for surfaces of table, cabinet, and chair, were much higher than their respective blanks, while the signal obtained for the doorknob was only slightly higher than its blank (Figure 4A-a). These differences may result from different physical properties of those surfaces, which affect the formation of sodium hypochlorite microcrystals (Figure S18). Overall, the BioChemPen allows one to realize if the daily use objects have been sanitized recently. In addition, we tested the surfaces of some food-related samples (Figure S16C,D) because some food supply companies disinfect fresh vegetables with sodium hypochlorite.[18] The results show that the BioChemPen can detect residual sodium hypochlorite on cucumber and enoki mushrooms (Figure S19). To further evaluate if analyte carryover occurred between analyses, we performed blank and sample analyses alternatively. After cleaning the sensing zone of the BioChemPen with Kimwipes, no carryover effect was observed between analyses (Figure S20).

**Detection of ATP and Evaluation of Meat Freshness Using Gel-Phase Luciferase Bioluminescent Reaction.** Detection of ATP is based on the luciferin−luciferase reaction[40] (Figure S1B). Because luciferin is the key substrate in this reaction, we tested its different concentrations within the range of $3.52 \times 10^{-4}$ to $2.11 \times 10^{-3}$ M and found $7.04 \times 10^{-4}$ M to be the optimum concentration (Figure S21A). As expected, this concentration is above the Michaelis constant ($11 \times 10^{-6}$ M) of luciferase from *Photinus pyralis* (E.C. 1.13.12.7) against luciferin.[41] The concentrations of the other chemicals (magnesium sulfate, EDTA, and luciferase) and the pH were based on previous work.[40]

To evaluate the quantitative capabilities of the described method, we prepared a calibration plot for different concentrations of ATP ($7.24 \times 10^{-13}$ to $1.63 \times 10^{-10}$ mol mm$^{-2}$; 10 levels) impregnated on filter paper disks (Figure 3B and Table 1). The LOD and LOQ [cf. formulae (1−3) in the Supporting Information] for ATP were $2.73 \times 10^{-13}$ and $9.09 \times 10^{-13}$ mol mm$^{-2}$, respectively. The repeatability (RSD = 5.94%, $n$ = 10; on one day) and the reproducibility (RSD = 7.20%, $n$ = 18; three replicates per day on six consecutive days) of the method were determined by detecting the ATP impregnated on the filter paper disks ($5.47 \times 10^{-11}$ mol mm$^{-2}$).

Because ATP is a major carrier of chemical energy in living organisms and plays a key role in cellular metabolism,[24] we intended to use the device to detect ATP on the meat surface to determine its freshness. Four kinds of meat (beef, pork, chicken, and salmon; Figure S22; cf. additional experimental details in the Supporting Information) were chosen for this experiment, and slices of ∼1 mm thickness were prepared prior to detection.



https://doi.org/10.1021/acssensors.1c01540
ACS Sens. 2021, 6, 3744−3752

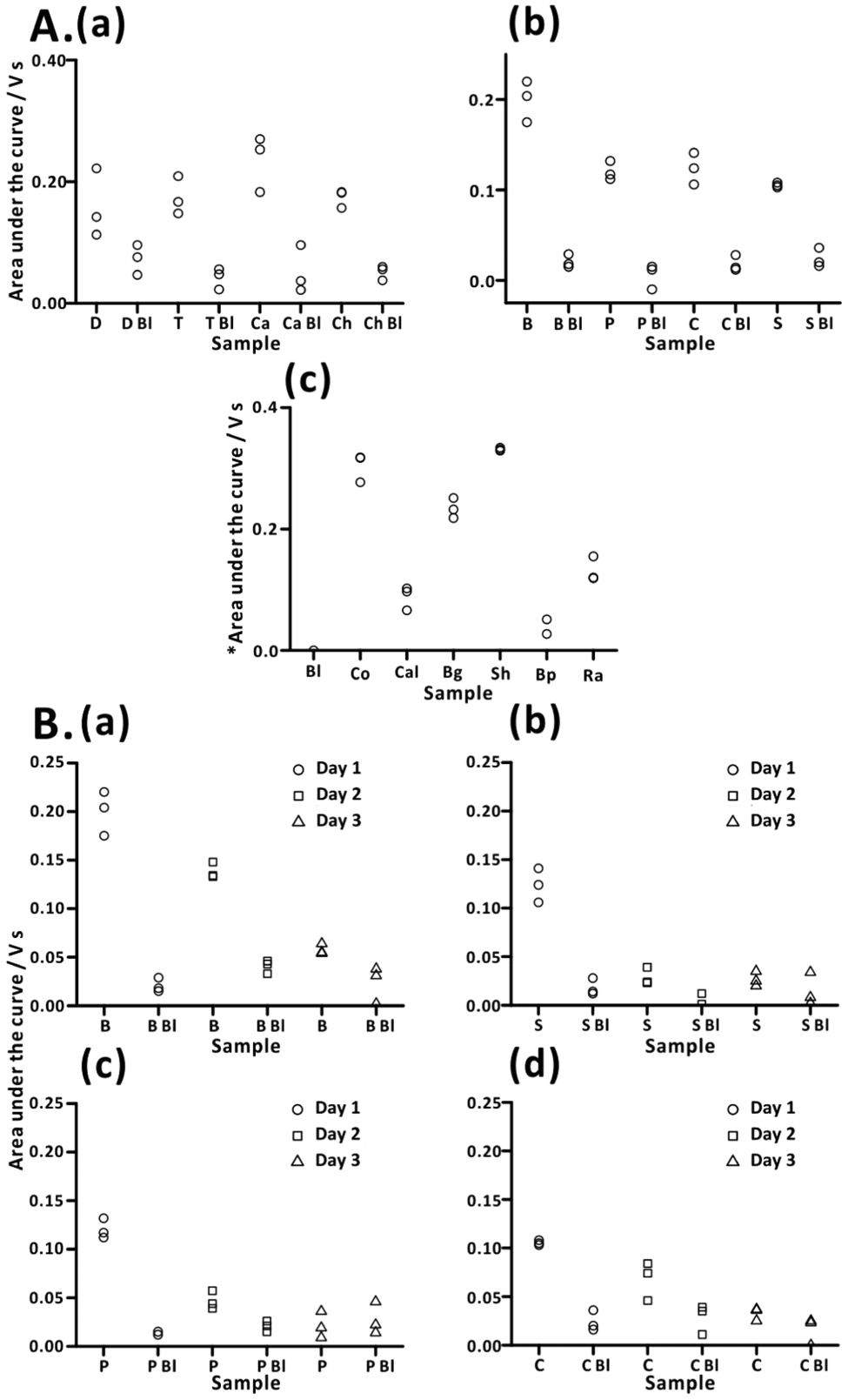


**Figure 4.** Real sample analysis with BioChemPen. (A): (a) bleach residue on solid surfaces (D, doorknob, T, table, Ca, cabinet, Ch, chair, Bl, blank); (b) ATP on the surface of the fresh meat (B, beef; P, pork; C, chicken; S, salmon; and Bl, blank); (c) pesticide residue on vegetables (Co, courgette; Cal, calabash; Bg, bitter gourd; Sh, shallots; Bp, bell pepper; Ra, radish; and Bl, blank); and (B) ATP on the surface of the meat stored for 1, 2, and 3 days [(a) beef, (b) pork, (c) chicken, and (d) salmon].

During the analysis, the luciferin−luciferase hydrogel was brought in direct contact with the surface of sliced meat. The analysis of the beef sample yielded the highest signal (Figure 4A-b; ATP concentration: $3.63 \times 10^{-12}$ mol mm$^{-2}$, $n = 3$) while the chicken, pork, and salmon samples yielded lower signals (<LOQ). Notably, a previous study[42] using a luminometer for



https://doi.org/10.1021/acssensors.1c01540
ACS Sens. 2021, 6, 3744−3752

the analysis of ATP in homogenized meat samples also reported higher ATP content for beef than for chicken, pork, and salmon samples. Furthermore, we stored the meat samples at room temperature for three consecutive days and evaluated their freshness by comparing the bioluminescence intensities for the analyses performed on each day (Figure 4B). The result shows that the ATP content in the meat samples reduced considerably on the second and the third day. It can be compared with the work by Nakatani et al.,[43] who also evaluated meat (beef and rabbit muscles) freshness as a function of time and observed changes in the amounts of ATP-related compounds such as ADP, adenosine monophosphate, inosine monophosphate, and hypoxanthine. There exist several other methods for verification of meat freshness (Table S1). The advantages of BioChemPen include convenience, straightforward operation, and no need for sample pretreatment. These are traded for the inability to quantify ATP inside meat cells. Also, note that the meat structure may have some effect on the availability of ATP for assay reaction, thus contributing to the matrix effect.

**Detection of ADP on Surfaces Using Gel-Phase Luciferase Bioluminescent Reaction Coupled with Pyruvate Kinase.** In the BioChemPen variant for detection of ADP, the target analyte is first converted to ATP by pyruvate kinase in the presence of PEP within the hydrogel, and then the ATP is detected using the luciferin−luciferase reaction[40] (Figure S1B). Different concentrations of PEP (0.001−0.006 M) were tested, and 0.001 M was found to be optimum (Figure S21B). Notably, this concentration is above the Michaelis constant (0.076 mM) of pyruvate kinase from rabbit muscle (E.C. 2.7.1.40) against PEP.[44] The concentrations of other chemicals (magnesium sulfate, EDTA, luciferase, and pyruvate kinase) were the same as previously reported.[40]

To evaluate the quantitative capabilities of the described method, we prepared a calibration plot for ADP ($4.09 \times 10^{-12}$ to $4.39 \times 10^{-11}$ mol mm$^{-2}$; 11 levels) impregnated on filter paper disks (Figure 3C and Table 1). The LOD and LOQ [cf. formulae (1−3) in the Supporting Information] for ADP were $2.35 \times 10^{-12}$ and $7.84 \times 10^{-12}$ mol mm$^{-2}$, respectively. The repeatability (RSD = 9.11%, $n$ = 10; on one day) and the reproducibility (RSD = 7.05%, $n$ = 18; three replicates per day on six consecutive days) of the method were determined with filter paper disks impregnated with ADP ($2.80 \times 10^{-11}$ mol mm$^{-2}$). It should be noted that the bioluminescence observed in this reaction during the analysis of real samples (e.g., meat) could correspond to the combined contribution of the sample's ADP and ATP.

**Detection of a Pesticide Using Gel-Phase Multienzyme Chemiluminescent Reaction.** To demonstrate the detection of a pesticide with BioChemPen, we implemented a multienzyme approach (Figure S1C) reported by Montali et al. for the detection of acetylcholinesterase inhibitors such as organophosphate pesticides.[45] Other methods available for the analysis of organophosphate pesticides are listed in Table S2. The AChE-ChOx-HRP hydrogel disk was first placed on a sample surface to collect organophosphate pesticide (chlorpyrifos-methyl) residues. Then, 10 $\mu$L of Ach solution was dropped on the hydrogel disk to generate hydrogen peroxide. Subsequently, the hydrogel disk was placed in the BioChemPen's cartridge and covered with a 3D-printed plastic cap (Figure S4) containing 10 $\mu$L of luminol solution to detect chemiluminescence. In this multienzyme assay, the production of hydrogen peroxide decreases because of the lack of AChE, which is inhibited by the pesticide. Several method conditions were optimized (Figures S23−S25), including the pH value of the Ach solution, the Ach concentration, the time of soaking AChE-ChOx-HRP hydrogel in the Ach solution, pH value of luminol, the luminol concentration, and the pesticide sampling time, and ratio of AChE to ChOx (for additional details see the Supporting Information).

To evaluate the quantitative capabilities of the described method, we prepared a calibration plot for chlorpyrifos-methyl ($2 \times 10^{-11}$ to $2 \times 10^{-9}$ mol mm$^{-2}$; 6 levels; Figure 3D and Table 1) deposited on glass slides. Because the area under the curve decreases with the increasing concentration of the inhibitor (chlorpyrifos-methyl) in this reaction, the calibration plot has a negative slope. However, to obtain a calibration curve with a positive slope for the calculation of LOD and LOQ values, we subtracted the area under the curve obtained for the standard sample test from that of the blank test (Figure 3D). The LOD and LOQ [cf. formulae (1−3) in the Supporting Information] for chlorpyrifos-methyl were $2.59 \times 10^{-10}$ and $8.64 \times 10^{-10}$ mol mm$^{-2}$, respectively. The repeatability (RSD = 9.19%, $n$ = 10; on one day) and the reproducibility (RSD = 8.63%, $n$ = 18; three replicates per day on six consecutive days) of the method were determined using $2 \times 10^{-9}$ mol mm$^{-2}$ chlorpyrifos-methyl deposited on glass slides. For real sample analysis, we tested the device for the detection of residual organophosphate pesticides on the surface of vegetables, including courgette, calabash, bitter gourd, shallots, bell pepper, and radish (Figure S26). The analyzed courgette and shallot samples showed the highest luminescence (Figure 4A-c), while the other samples showed lower signals (<LOQ). Using the calibration equation, the concentrations of pesticide in courgette and shallot samples were calculated to be $1.03 \times 10^{-9}$ mol mm$^{-2}$ ($n$ = 3) and $1.09 \times 10^{-9}$ mol mm$^{-2}$ ($n$ = 3), respectively.

**Hydrogel Storage.** The stability of hydrogel disks was investigated by simulating storage and shipment conditions. The hydrogel storage modules (Figure S27) were printed using a 3D printer and vacuum-packed in the plastic bags by employing a simple commercial vacuum machine used for food preservation. The vacuum-sealed packs, placed in a plastic container, were stored at 4 °C. In the tests involving storage of luminol−hydrogen peroxide hydrogel, luciferin−luciferase hydrogel, and luciferin−luciferase−pyruvate kinase hydrogel (cf. Experimental Section), the luminescence decreased with increasing storage times (Figure S28). Therefore, it is suggested to utilize these types of hydrogels within 3 days from the day of their preparation. On the other hand, the AChE-ChOx-HRP hydrogel was not stable for a long time (>10 min). Hence, to ensure reliable quantitative analysis, it is recommended to prepare fresh AChE-ChOx-HRP hydrogel before analyses.

## CONCLUSIONS

We have developed BioChemPen, a miniature handheld cloud-integrated device for the detection of chemical residues supported on solid surfaces. The device has been built with an MCB, a handful of low-cost electronic components, and accessible prototyping tools. The sensing principle relies on gel-phase reactions that exhibit (bio)chemiluminescence. Four different reactions have been demonstrated: luminol, luciferase, luciferase−pyruvate kinase, and luminol−enzyme reactions. The device can be used to detect residual bleach on solid surfaces, evaluate the freshness of meat, and detect residual pesticides on surfaces of vegetables. The main limitation of the method is the limited stability of the hydrogel. Drying of the hydrogel and denaturation of the enzyme(s) over time may


https://doi.org/10.1021/acssensors.1c01540
ACS Sens. 2021, 6, 3744−3752

adversely influence the results. Lastly, in line with the Internet-of-Chemical-Things,[46,47] the concept of BioChemPen can be used to build networks of distributed sensors, in which large amounts of chemical data will flow to a central database and become available for immediate interpretation.

## ■ ASSOCIATED CONTENT

### Supporting Information

The Supporting Information is available free of charge at https://pubs.acs.org/doi/10.1021/acssensors.1c01540.

Additional experimental details (chemicals; calculation of LOD and LOQ; real samples); description of additional results (optimization of reaction conditions for the detection of pesticide); additional tables (S1−S2); additional figures (S1−S28); and MicroPython PyBoard codes; tables present a comparison of different methods; figures present additional details of BioChemPen and results, such as reaction schemes; technical drawings and photographs of BioChemPen and related components; illustration of cloud-integration features; protocol for preparation of hydrogel disks; photographs of sampled surfaces; optimization results; real sample analysis results; and hydrogel storage test results (PDF)

Video illustrates the operation of BioChemPen (Movie S1) (MP4)

## ■ AUTHOR INFORMATION


### Corresponding Author

**Pawel L. Urban** − *Department of Chemistry, National Tsing Hua University, Hsinchu 30013, Taiwan; Frontier Research Center on Fundamental and Applied Sciences of Matters, National Tsing Hua University, Hsinchu 30013, Taiwan;* orcid.org/0000-0003-3471-045X; Email: urban@mx.nthu.edu.tw

### Authors

**Yu-Ting Chao** − *Department of Chemistry, National Tsing Hua University, Hsinchu 30013, Taiwan*

**Gurpur Rakesh D. Prabhu** − *Department of Chemistry, National Tsing Hua University, Hsinchu 30013, Taiwan;* orcid.org/0000-0002-3237-212X

**Kai-Chiang Yu** − *Department of Chemistry, National Tsing Hua University, Hsinchu 30013, Taiwan*

**Jia-You Syu** − *Department of Chemistry, National Tsing Hua University, Hsinchu 30013, Taiwan*

Complete contact information is available at: https://pubs.acs.org/10.1021/acssensors.1c01540


### Notes

The authors declare no competing financial interest.

## ■ ACKNOWLEDGMENTS

We acknowledge the Ministry of Science and Technology (MOST), Taiwan (grant numbers 109-2113-M-007-013-MY3, 110-2634-F-007-023, and 110-2811-M-007-502), the National Tsing Hua University (110QI009E1), and the Frontier Research Center on Fundamental and Applied Sciences of Matters as well as the Featured Areas Research Center Program within the framework of the Higher Education Sprout Project established by the Ministry of Education (MOE), Taiwan (110QR001I5). We also thank En-Cih Lee, Yi-Wun Wang, and Decibel P. Elpa for their assistance.

## ■ REFERENCES


(1) Zhang, D.; Liu, Q. Biosensors and Bioelectronics on Smartphone for Portable Biochemical Detection. *Biosens. Bioelectron.* **2016**, *75*, 273−284.

(2) Wang, S. Q.; Chinnasamy, T.; Lifson, M. A.; Inci, F.; Demirci, U. Flexible Substrate-Based Devices for Point-of-Care Diagnostics. *Trends Biotechnol.* **2016**, *34*, 909−921.

(3) Tu, J.; Torrente-Rodríguez, R. M.; Wang, M.; Gao, W. The Era of Digital Health: A Review of Portable and Wearable Affinity Biosensors. *Adv. Funct. Mater.* **2020**, *30*, No. 1906713.

(4) Garzón, V.; Pinacho, D. G.; Bustos, R.-H.; Garzón, G.; Bustamante, S. Optical Biosensors for Therapeutic Drug Monitoring. *Biosensorsl* **2019**, *9*, No. 132.

(5) Lukyanenko, K. A.; Denisov, I. A.; Sorokin, V. V.; Yakimov, A. S.; Esimbekova, E. N.; Belobrov, P. I. Handheld Enzymatic Luminescent Biosensor for Rapid Detection of Heavy Metals in Water Samples. *Chemosensors* **2019**, *7*, No. 16.

(6) Kassal, P.; Steinberg, M. D.; Steinberg, I. M. Wireless Chemical Sensors and Biosensors: A Review. *Sens. Actuators, B* **2018**, *266*, 228−245.

(7) Baldock, J. D. Microbiological Monitoring of the Food Plant: Methods to Assess Bacterial Contamination on Surfaces. *J. Milk Food Technol.* **1974**, *37*, 361−368.

(8) Anderson, B. M. *Prevention and Control of Infections in Hospitals: Practice and Theory*; Springer: Berlin, 2019.

(9) Arena, A. DNA Exitus Plus Versus Standard Bleach Solution for the Removal of DNA Contaminants on Work Surfaces and Tools. *Invest. Sci. J.* **2010**, *2*, 20−29.

(10) Suman, R.; Javaid, M.; Haleem, A.; Vaishya, R.; Bahl, S.; Nandan, D. Sustainability of Coronavirus on Different Surfaces. *J. Clin. Exp. Hepatol.* **2020**, *10*, 386−390.

(11) Kohli, R.; Mittal, K. L. Methods for Assessing Surface Cleanliness. In *Developments in Surface Contamination and Cleaning, Volume 12: Methods for Assessment and Verification of Cleanliness of Surfaces and Characterization of Surface Contaminants*; Elsevier: Amsterdam, 2019; Chapter 3, pp 23−105.

(12) Hall, L. B.; Hartnett, M. J. Measurement of the Bacterial Contamination on Surfaces in Hospitals. *Public Health Rep.* **1964**, *79*, 1021−1024.

(13) Whitfield, W. J.; Beakley, J. W.; Dugan, V. L.; Hughes, L. W.; Morris, M. E.; McDade, J. J. Vacuum Probe: New Approach to the Microbiological Sampling of Surfaces. *Appl. Microbiol.* **1969**, *17*, 164−168.

(14) Aycicek, H.; Oguz, U.; Karci, K. Comparison of Results of ATP Bioluminescence and Traditional Hygiene Swabbing Methods for the Determination of Surface Cleanliness at a Hospital Kitchen. *Int. J. Hyg. Environ. Health* **2006**, *209*, 203−206.

(15) Mafu, A. A.; Pitre, M.; Sirois, S. Real-Time PCR as a Tool for Detection of Pathogenic Bacteria on Contaminated Food Contact Surfaces by Using a Single Enrichment Medium. *J. Food Prot.* **2009**, *72*, 1310−1314.

(16) Kohli, R. Methods for Monitoring and Measuring Cleanliness of Surfaces. In *Developments in Surface Contamination and Cleaning: Detection, Characterization, and Analysis of Contaminants*; Kohli, R.; Mittal, K. L., Eds.; William Andrew: Norwich, 2012; Vol. *4*, pp 107−178.

(17) Francisco, C. A. I.; Naves, E. A. A.; Ferreira, D. C.; Do Rosário, D. K. A.; Cunha, M. F.; Bernardes, P. C. Synergistic Effect of Sodium Hypochlorite and Ultrasound Bath in the Decontamination of Fresh Arugulas. *J. Food Saf.* **2018**, *38*, No. e12391.

(18) Gil, M. I.; Marín, A.; Andujar, S.; Allende, A. Should Chlorate Residues be of Concern in Fresh-Cut Salads? *Food Control* **2016**, *60*, 416−421.

(19) Garrido, Y.; Marín, A.; Tudela, J. A.; Allende, A.; Gil, M. I. Chlorate Uptake During Washing is Influenced by Product Type and Cut Piece Size, as well as Washing Time and Wash Water Content. *Postharvest Biol. Technol.* **2019**, *151*, 45−52.

(20) Herrero, A. M. Raman Spectroscopy a Promising Technique for Quality Assessment of Meat and Fish: A Review. *Food Chem.* **2008**, *107*, 1642−1651.
(21) Kamruzzaman, M.; Makino, Y.; Oshita, S. Non-Invasive Analytical Technology for the Detection of Contamination, Adulteration, and Authenticity of Meat, Poultry, and Fish: A Review. *Anal. Chim. Acta* **2015**, *853*, 19−29.
(22) Li, Z.; Suslick, K. S. Portable Optoelectronic Nose for Monitoring Meat Freshness. *ACS Sens.* **2016**, *1*, 1330−1335.
(23) Liu, Z.; Zhong, Y.; Hu, Y.; Yuan, L.; Luo, R.; Chen, D.; Wu, M.; Huang, H.; Li, Y. Fluorescence Strategy for Sensitive Detection of Adenosine Triphosphate in Terms of Evaluating Meat Freshness. *Food Chem.* **2019**, *270*, 573−578.
(24) Berg, J. M. Metabolism: Basic Concepts and Design. In *Biochemistry*, 7th ed.; W.H. Freeman & Company: New York, 2010.
(25) Lozowicka, B. Health Risk for Children and Adults Consuming Apples with Pesticide Residue. *Sci. Total Environ.* **2015**, *502*, 184−198.
(26) Stachniuk, A. LC-MS/MS Determination of Pesticide Residues in Fruits and Vegetables. In *Bioactive Molecules in Food*; Mérillon, J.-M.; Ramawat, K. G., Eds.; Springer: Cham, 2019; pp 2137−2161.
(27) Štajnbaher, D.; Zupančič-Kralj, L. Multiresidue Method for Determination of 90 Pesticides in Fresh Fruits and Vegetables Using Solid-Phase Extraction and Gas Chromatography-Mass Spectrometry. *J. Chromatogr. A* **2003**, *1015*, 185−198.
(28) Caló, E.; Khutoryanskiy, V. V. Biomedical Applications of Hydrogels: A Review of Patents and Commercial Products. *Eur. Polym. J.* **2015**, *65*, 252−267.
(29) Ullah, F.; Othman, M. B. H.; Javed, F.; Ahmad, Z.; Akil, H. M. Classification, Processing and Application of Hydrogels: A Review. *Mater. Sci. Eng., C* **2015**, *57*, 414−433.
(30) Luchini, A.; Geho, D. H.; Bishop, B.; Tran, D.; Xia, C.; Dufor, R. L.; Jones, C. D.; Espina, V.; Patanarut, A.; Zou, W.; et al. Smart Hydrogel Particles: Biomarker Harvesting: One-Step Affinity Purification, Size Exclusion, and Protection against Degradation. *Nano Lett.* **2008**, *8*, 350−361.
(31) Ahmad, E. M. Hydrogel: Preparation, Characterization, and Applications: A Review. *J. Adv. Res.* **2015**, *6*, 105−121.
(32) Walker, N. L.; Dick, J. E. Oxidase-loaded hydrogels for versatile potentiometric metabolite sensing. *Biosens. Bioelectron.* **2021**, *178*, No. 112997.
(33) MicroPython. https://micropython.org (accessed May 20, 2021).
(34) Urban, P. L. Universal Electronics for Miniature and Automated Chemical Assays. *Analyst* **2015**, *140*, 963−975.
(35) Urban, P. L. Prototyping Instruments for the Chemical Laboratory Using Inexpensive Electronic Modules. *Angew. Chem., Int. Ed.* **2018**, *57*, 11074−11077.
(36) Prabhu, G. R. D.; Yang, T.-H.; Hsu, C.-Y.; Shih, C.-P.; Chang, C.-M.; Liao, P.-H.; Ni, H.-T.; Urban, P. L. Facilitating Chemical and Biochemical Experiments with Electronic Microcontrollers and Single-Board Computers. *Nat. Protoc.* **2020**, *15*, 925−990.
(37) Prabhu, G. R. D.; Urban, P. L. Elevating Chemistry Research with a Modern Electronics Toolkit. *Chem. Rev.* **2020**, *120*, 9482−9553.
(38) Seitz, W. R. Chemiluminescence from the Reaction between Hypochlorite and Luminol. *J. Phys. Chem. A* **1975**, *79*, 101−106.
(39) World Health Organization. Cleaning and Disinfection of Environmental Surfaces in the Context of Covid-19: Interim Guidance. https://apps.who.int/iris/handle/10665/332096 (accessed June 26, 2021).
(40) Liu, P.-H.; Urban, P. L. Spontaneous Luminescence Color Change in the Firefly Luciferase Assay System. *Anal. Biochem.* **2017**, *539*, 54−59.
(41) Moradi, A.; Hosseinkhani, S.; Naderi-Manesh, H.; Sadeghizadeh, M.; Alipour, B. S. Effect of Charge Distribution in a Flexible Loop on the Bioluminescence Color of Firefly Luciferases. *Biochemistry.* **2009**, *48*, 575−582.
(42) Bakke, M.; Suzuki, S. Development of a Novel Hygiene Monitoring System Based on the Detection of Total Adenylate (ATP +ADP+AMP). *J. Food Prot.* **2018**, *81*, 729−737.
(43) Nakatani, Y.; Fujita, T.; Sawa, S.; Otani, T.; Hori, Y.; Takagahara, I. Changes in Atp-Related Compounds of Beef and Rabbit Muscles and a New Index of Freshness of Muscle. *Agric. Biol. Chem.* **1986**, *50*, 1751−1856.
(44) Boehme, C.; Bieber, F.; Linnemann, J.; Breitling, R.; Lorkowski, S.; Reissmann, S. Chemical and Enzymatic Characterization of Recombinant Rabbit Muscle Pyruvate Kinase. *Biol. Chem.* **2013**, *394*, 695−701.
(45) Montali, L.; Calabretta, M. M.; Lopreside, A.; D'Elia, M.; Guardigli, M.; Michelini, E. Multienzyme Chemiluminescent Foldable Biosensor for on-Site Detection of Acetylcholinesterase Inhibitors. *Biosens. Bioelectron.* **2020**, *162*, No. 112232.
(46) Ley, S. V.; Fitzpatrick, D. E.; Ingham, R. J.; Nikbin, N. The Internet of Chemical Things. *Beilstein Mag.* **2015**, *1*, No. 2.
(47) Prabhu, G. R. D.; Witek, H. A.; Urban, P. L. Telechemistry: Monitoring Chemical Reactions via the Cloud Using the Particle Photon Wi-Fi Module. *React. Chem. Eng.* **2019**, *4*, 1616−1622.


https://doi.org/10.1021/acssensors.1c01540
*ACS Sens.* 2021, 6, 3744−3752